© Pol J Radiol 2023; 88: e435-e444
DOI: https://doi.org/10.5114/pjr.2023.131000

Received: 28.07.2023
Accepted: 01.08.2023
Published: 22.09.2023

Polish Journal of Radiology

http://www.polradiol.com

Review paper

3D computed tomography intravascular endoscopy

Haris Huseinagić[1,A,B,D,E], Alma Efendić[1,A,F], Irma Rušidović[2,A,F]

[1]Medical Institute Bayer in Tuzla, Bosnia and Herzegovina
[2]Pharmamaac d.o.o., Bosnia and Herzegovina

Abstract

Using coronary computed tomography angiography (CCTA), coronary plaques can be characterized based on both their morphology and composition. Coronary plaques are generally assessed on 2D axial and multiplanar reformatted images. Nevertheless, these visualization tools are limited to observing extraluminal changes in the coronary artery. The presence of plaques prevents them from providing a visual representation of the intraluminal coronary wall. Since its invention in 2000, coronary fly-through or virtual angioscopy (VA) has been extensively studied. However, its application was limited because it required an optimal CT scan and time-consuming post-processing. In recent years, advances in post-processing software have made construction of VA easier, but until recently the quality of the images was insufficient for most patients. Using 3D intravascular endoscopy (3DIE) visualization, we present various intraluminal appearances of the coronary wall and plaque in relation to various types of plaque.

Key words: coronary CT angiography, coronary artery disease, plaque, 3D intravascular endoscopy, visualization.

Introduction

Coronary computed tomography angiography (CCTA) is a well-established, less invasive imaging modality for the diagnosis of coronary artery disease (CAD), with many studies reporting its high diagnostic value [1-5]. CCTA can characterize coronary plaques in terms of plaque components, in addition to detecting and assessing coronary artery stenosis [6-8]. It is generally agreed that the composition of the plaque, rather than the degree of luminal narrowing, provides more accurate information for predicting the patient's risk of future cardiac events [1].

Since its first mention in 2000, coronary fly-through or 3D intravascular endoscopy (3DIE) using various generations of computed tomography (CT) devices has been reported in a number of publications [9,10]. The main reason for the limited research done on this subject was the requirement of an optimal CT scan and time-consuming post-processing. Recent advancements in post-processing software have made 3DIE construction easier. Because of its higher temporal resolution, the introduction of multidetector CT (MDCT) has provided a more stable quality of data in all patients.

Coronary plaques are commonly assessed using 2D axial and multiplanar reformatted images, in addition to 3D volume rendering images. The main limitation of these visualizations is the lack of direct intraluminal views of plaque appearances and associated coronary wall changes. This limitation is overcome by 3DIE, a 3D visualization technique with proven diagnostic application in cardiovascular disease [11-15].

Correspondence address:
Haris Huseinagić, Medical Institute Bayer in Tuzla, Bosnia and Herzegovina, e-mail: hmirma95@gmail.com

Authors' contribution:
A Study design · **B** Data collection · **C** Statistical analysis · **D** Data interpretation · **E** Manuscript preparation · **F** Literature search · **G** Funds collection

Material and methods

A total of 121 patients (95 males, mean age 60 ± 13 years) were selected at random from patients who had their coronary arteries scanned on an MDCT using a standard coronary artery protocol (uWS-CT Workstation, Shanghai United Imaging Healthcare Co. Ltd.).

Allergy to iodine-containing contrast medium, renal insufficiency (creatinine level > 120 µmol/l), pregnancy, haemodynamic instability, and previous stent graft or bypass surgery were all exclusion criteria for DSCT.

The study did not exclude patients with elevated or irregular heart rates. Our local Ethics Committee approved the study protocol, and all patients who took part provided written informed consent.

No β-blockers were administered prior to the scan, except for patients with a heart rate above 90 bpm.

In all patients, CCTA was performed with retrospective ECG gating on a 160-multislice (MSCT) CT (uCT 780, Shanghai United Imaging Healthcare Co. Ltd.).

Non-invasive coronary angiography and virtual coronary angioscopy

We used a uCT 780 scanner (Shanghai United Imaging Healthcare Co. Ltd.) with a 512 × 512 reconstruction matrix and ECG-gated heart phase selective image reconstruction for MSCT. A total of 90 ml of contrast agent (370 mg/ml) was injected through an 18-gauge catheter into an antecubital vein at 4 ml/s, followed by 30 ml of saline for the contrast-enhanced scan (collimation 1.0 mm; pitch 1.5, 120 kV, 300 mA; rotation time 500 ms) [16].

All scans were carried out during a single 5-second breath hold. The raw scan data was then reconstructed using ECG-gated multislice spiral reconstruction algorithms [16]. In a test series, the timepoint for optimized image reconstruction was determined. In our series, image reconstruction was performed during the diastolic phase, with a 38-50% delay after the onset of the R wave for the right coronary artery and a 50% delay for the left coronary artery, using retrospective ECG gating. With a 0.625 mm slice increment and a matrix size of 512 × 512, 150 to 200 axial image slices were reconstructed, covering the entire volume of the heart with an almost isotropic spatial resolution (0.25 × 0.25 × 0.5 mm).

The image reconstruction field of view was tailored to the heart volume (range 150-200 mm), resulting in pixel sizes ranging from 0.29 × 0.29 mm to 0.39 × 0.39 mm. The image data were reconstructed and transferred to a computer workstation for postprocessing (uWS-CT Workstation Shanghai United Imaging Healthcare Co. Ltd.). When performing 3-dimensional volume rendering, image data are transferred into 3-dimensional voxels, each of which has a different density value expressed in Hounsfield units (HU).

Simultaneous display of CCTA report, CT IVUS, multiplanar reformatted (MPR 3-dimensional volume rendered models), 3D flow analysis, and endoscopic view enable precise interactive viewpoint navigation (Figure 1). The navigator is first placed in the region of interest; automatic path definition then finds the most direct path from one target point to another, giving the impression of flying through the vessel lumen of the coronary arteries.

The scanning protocols for these CT scanners were as follows: detector collimation 2 × 32 × 0.6 mm, gantry rotation 0.33 s, tube voltage 100-120 kVp depending on body mass index (BMI) and tube current ranging 345-420 mAs/rot; detector collimation 160 × 0.5 mm, gantry rotation of 0.3 s, tube voltage 100-120 kVp depending on BMI and automatic tube current modulation for the 160-slice CT. β-blockers were administered in patients with heart rate more than 90 bpm (beats per minute) for 160-slice CT.

Lopromide (370 mg/ml, Bayer Schering Pharma) was injected using a dual-head power injector with bolus tracking technique and a CT attenuation of 130 HU as the triggering threshold in the ascending aorta to initiate the scan. In the 120 kV protocol, 90 ml of contrast medium was injected at a rate of 4.5-5.5 ml/s. All injections were followed by a 30 ml saline flush. ECG tube current modulation was used with full tube current from 30% to 75% of the R-R interval. For DSCT protocols, the pitch ranged from 0.2 to 0.4 and was determined by heart rate. For DSCT, images were reconstructed with 0.6-0.75 mm slice thickness and 0.5-0.6 mm increments.

Post-processing was performed on a uWS-CT Workstation (Shanghai United Imaging Healthcare Co. Ltd.). The software allows a semiautomatic small vessel fly-through, which provides inside front and rear views, together with a view of the path and location on the surface of the heart (Figure 2). Besides this, 3 multiplanar reformation planes (sagittal, coronal, and axial) are shown for the location of the camera. The length travelled per major branch was recorded in millimetres, together with the time required in minutes to perform the evaluation per major branch. Ostia of side branches were visualized, but no fly-through of those side branches was performed.

CCTA findings in coronary artery disease and coronary stenting

Coronary plaques were most commonly found in the left anterior descending (LAD) coronary artery in 42 patients (35%), the LAD and left circumflex (LCX) in 30 patients (25%), all 3 main coronary vessels in 24 patients (20%), and the right coronary artery (RCA) in 12 patients (10%). In the remaining 13 patients (10%), plaques involving both the LAD and the RCA were discovered.

CCTA findings with patent coronary stents were found to be normal in 10 of 16 patients treated with coronary stents, while in-stent restenosis was suspected in

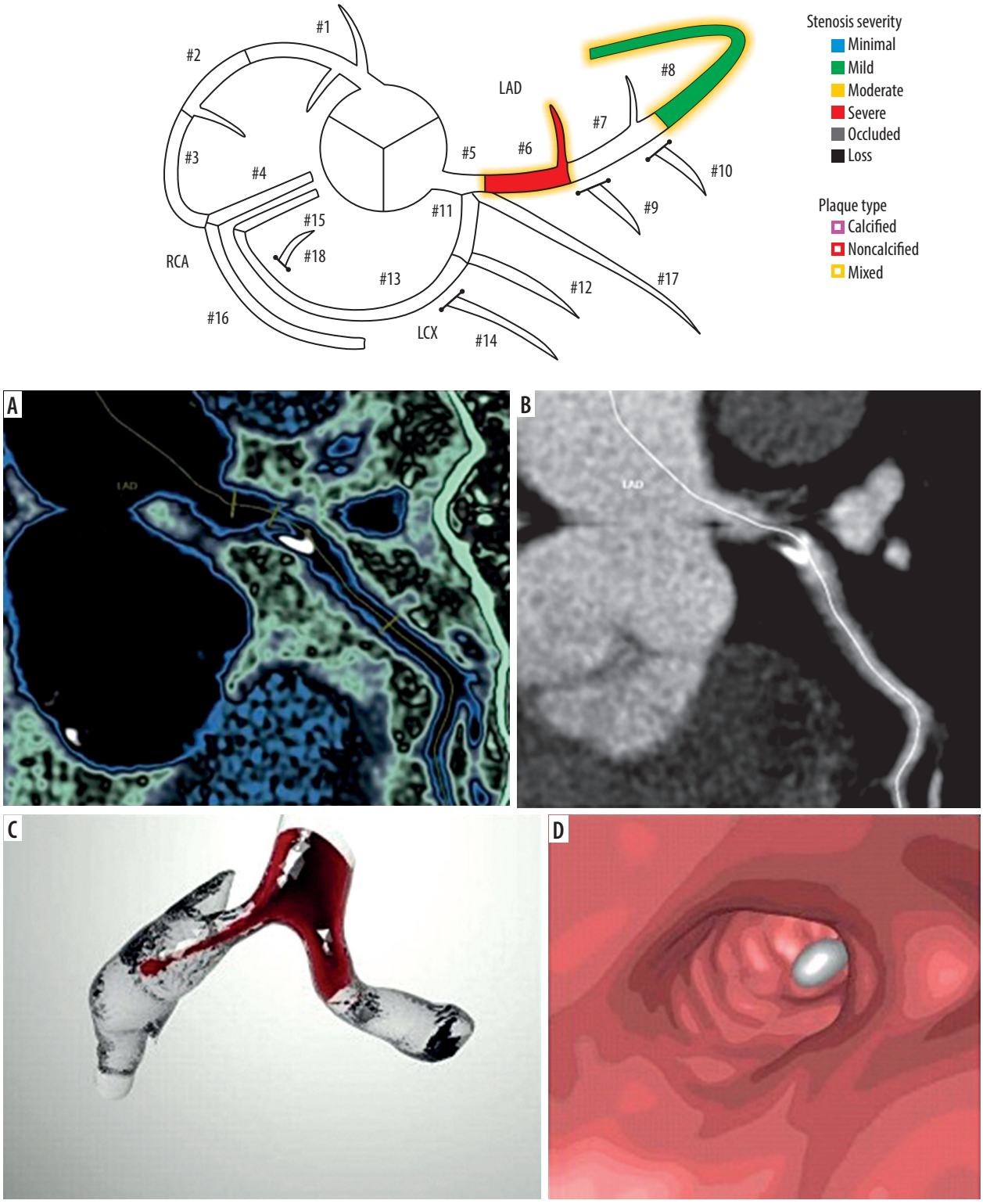

Figure 1. Correlation of VIE visualization and orthogonal views of coronary anatomy and plaque. Report sample (**A**), CTIVUS (**B**) and curved planar reformatted image (**C**) of the segment #6 LAD with mixed plaque, thrombus, and calcium. 3D model with flow analysis of noncalcified stenosis (**D**)

the remaining 6 patients. A total of 11 stents were placed in the coronary arteries of 10 patients with patent stents, with 7 in the LAD, 3 in the RCA, and one in the LCX. A total of 6 stents were placed in the coronary arteries of 5 patients with suspected in-stent restenosis, 3 in the LAD, 2 in the LCX, and one in the RCA (Table 1).

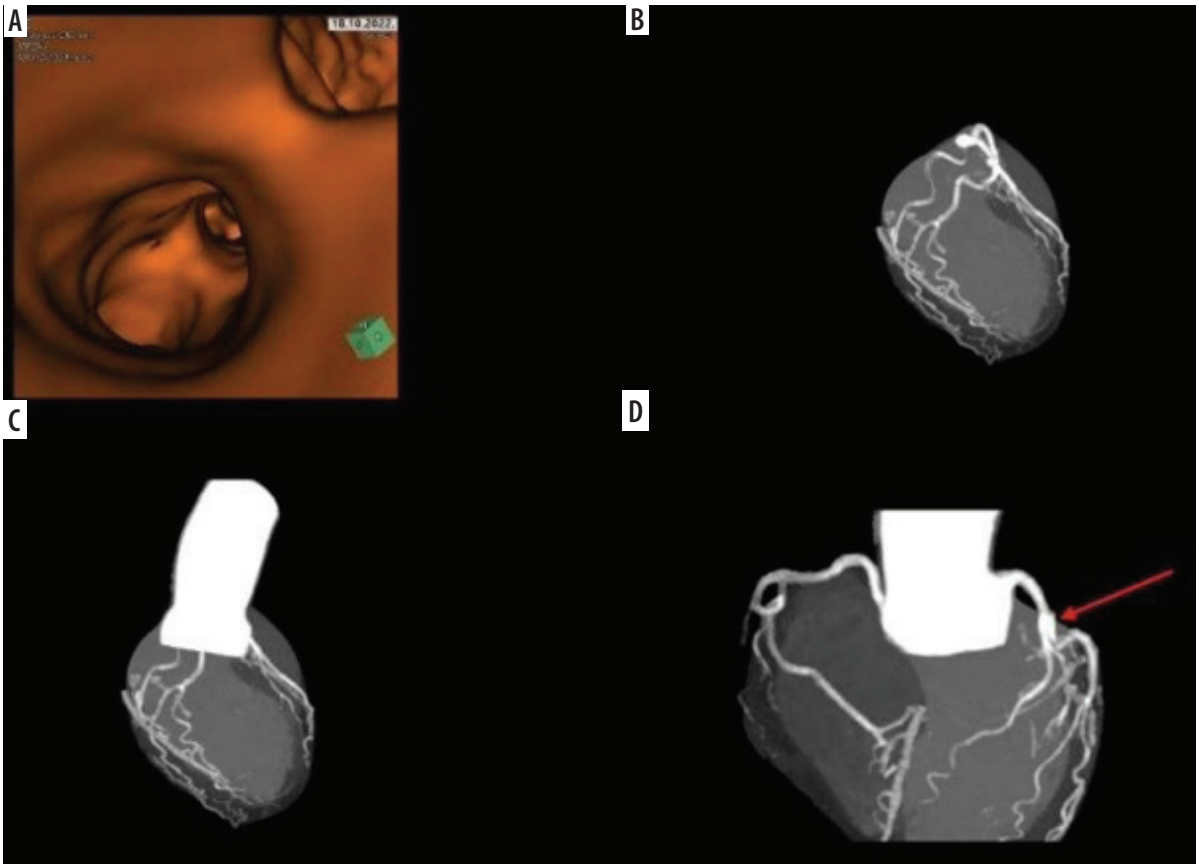

Figure 2. The software allows a semiautomatic small vessel fly-through, which provides inside front and rear views, together with a view of the path and location on the surface of the heart

Table 1. Patients' characteristics and cardiovascular risk factors

Parameter	Data
Age (years), mean (SD); range	57 (10); 41-71
Male sex (%)	82
Smoking (%)	66
Diabetes mellitus (%)	25
Hyperlipidaemia (%)	74
Hypertension (%)	69
Body mass index (kg/m^2), mean (SD)	28 (3)
Family history (%)	45

3D intravascular endoscopy image generation

CT volume data were generated from original DICOM images and transferred to a workstation running uWS-CT version R004 (Shanghai United Imaging Healthcare Co. Ltd.) for 3DIE image generation.

The CT data were post-processed using a CT number thresholding technique [17]. In summary, the first step was to measure CT attenuation at the main coronary arteries, specifically the right and left coronary arteries, to determine the threshold used to remove the contrast-enhanced blood from the coronary artery. The CT threshold value, which was determined in the first step to be between 200 and 350 HU, was then used to generate intraluminal views of coronary artery ostium, lumen surface, and coronary plaques. After determining an averaged threshold, the upper threshold was gradually increased in 20-HU increments to detect changes in the coronary wall and plaque surface.

This prevents floating shapes and other artifacts from appearing in the final 3DIE images. If an inappropriate threshold is chosen, the intraluminal appearance of the coronary ostium or plaque may be irregular or distorted due to the presence of artifacts, affecting visualization and assessment of coronary lesions.

Because the coronary artery is relatively small in diameter (3-5 mm), the intraluminal appearance of the coronary ostium and plaques visualized on 3DIE images must be correlated with corresponding orthogonal views to verify the exact anatomic details (Figure 3). This ensures that both normal anatomic structures and abnormal wall changes are correctly identified.

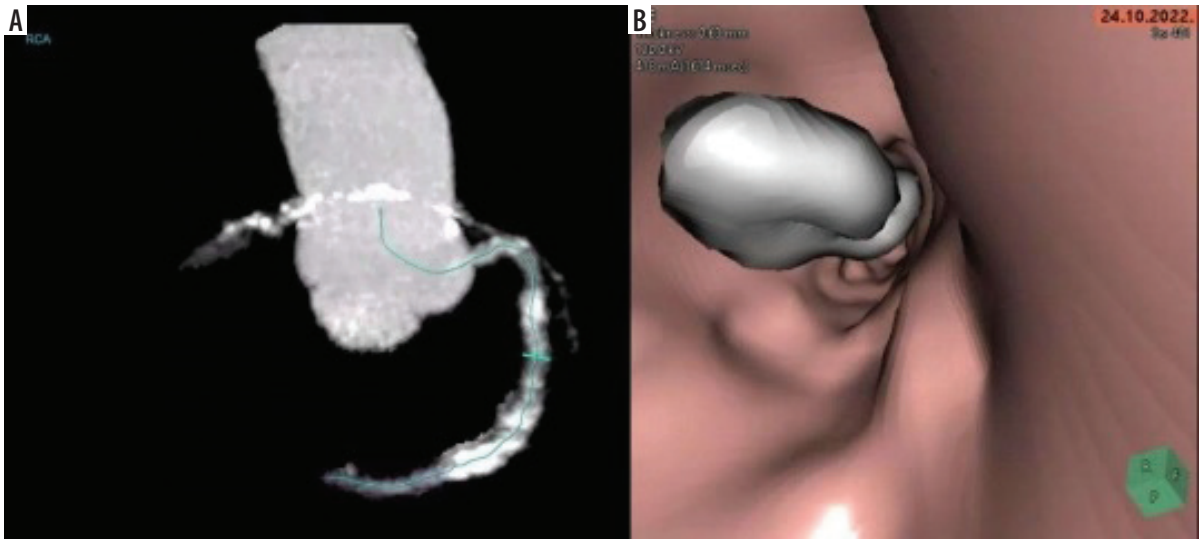

Figure 3. 3D IE visualization of non-calcified plaque. **A**) Curved planar reformatted image shows noncalcified plaque (arrow) at the proximal segment of LAD in a 67-year-old man. **B**) Corresponding 3D IE shows the plaque arising from the inferior wall of LAD with smooth appearance

Normal coronary artery wall 3DIE appearances

On 3DIE, the coronary wall appears smooth, with clear demonstration of the coronary ostial configuration and lumen in a normal coronary artery without the presence of coronary plaques or atherosclerotic changes. Figure 4 depicts the normal intraluminal appearance of left coronary ostia corresponding to various branches arising from the left coronary artery and the normal right coronary ostium as seen on 3DIE visualization.

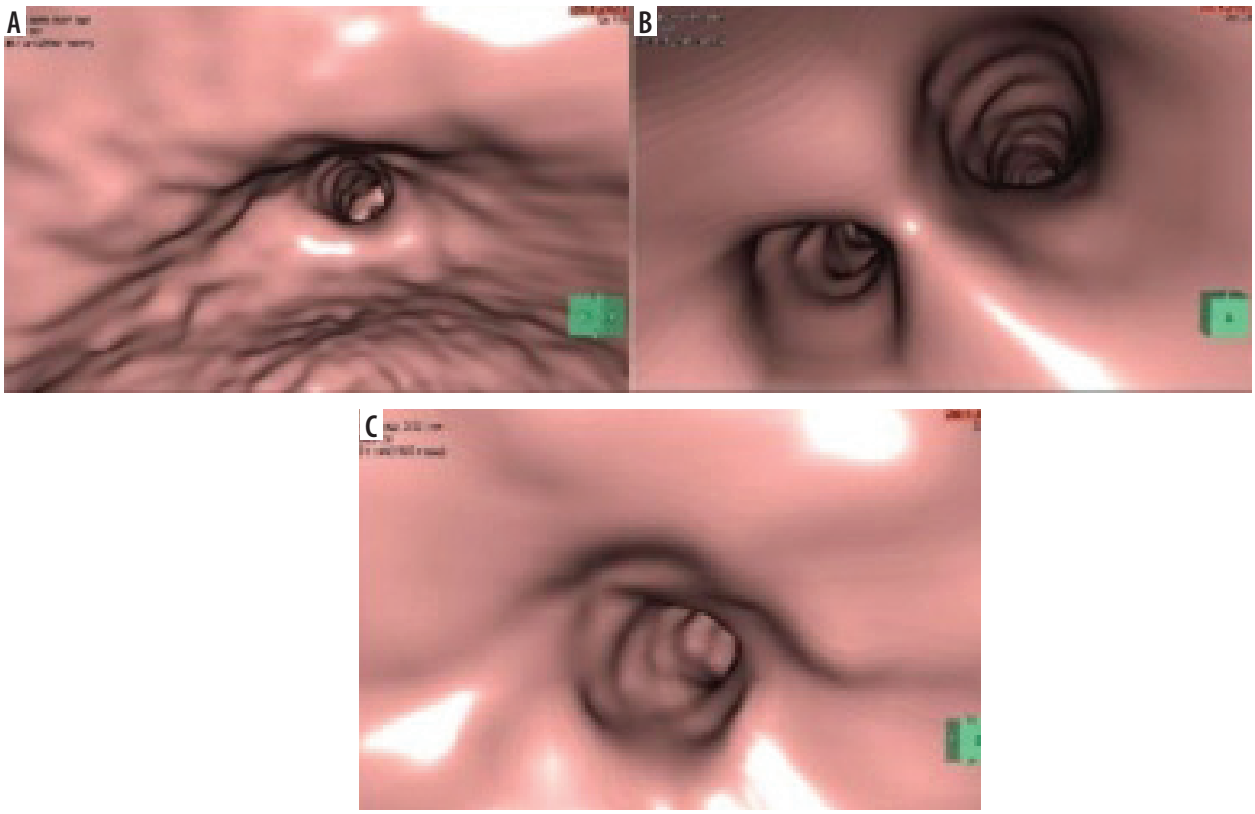

Figure 4. The normal intraluminal appearance of the left main artery (**A**), left coronary ostia corresponding to various branches arising from the left coronary artery (**B**), and the normal right coronary ostium (**C**) as seen on (3DIE) visualization

Coronary plaque 3DIE appearance

The appearance of plaques and the subsequent changes in the coronary wall are determined by the type, composition, and extent of the plaques. Furthermore, the plaques' position or location in relation to the artery wall can be evaluated in terms of eccentric or concentric appearances, as well as whether the coronary ostium is covered by the plaques or not.

The following sections show (3DIE) the appearances associated with various types of plaques.

Plaques that have not calcified

Non-calcified plaques are frequently seen on 3DIE as a smooth, protruding sign emanating from the coronary wall (Figure 5). Because CT attenuation of non-calcified plaque is much lower than that of contrast-enhanced blood in the coronary artery, changing the CT threshold when the viewing position is moved from the normal coronary artery to the location where plaque is located is important for demonstrating the non-calcified plaque in relation to the surrounding coronary artery ostia.

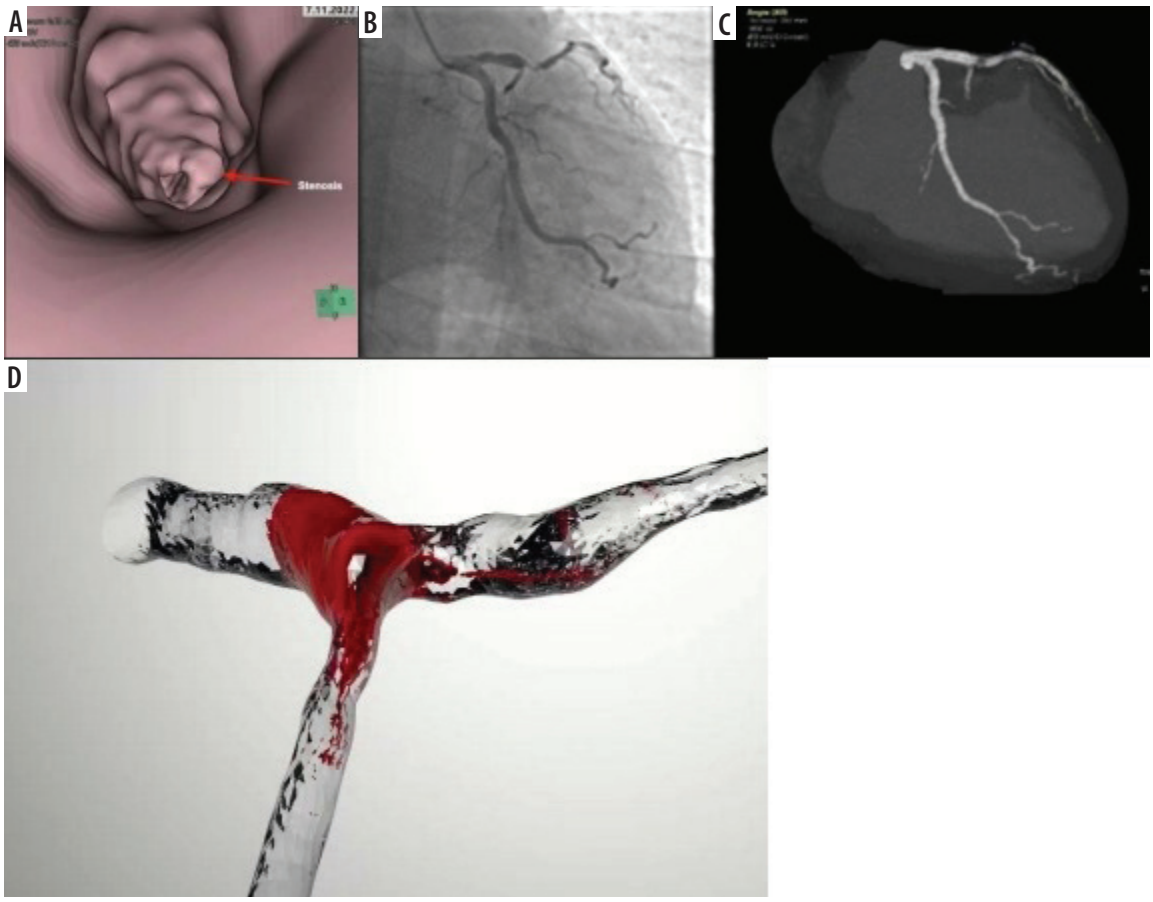

Figure 5. 3D IE visualization of non-calcified plaque (**A**). DSA and curved planar reformatted image shows non-calcified plaque at the proximal segment (segment #7) of LAD in a 52-year-old male (**B**). 3D model with flow analysis of noncalcified stenosis (**C**)

Plaques that have been calcified

On 3DIE, calcified plaques are typically depicted as a protruding sign with a smooth appearance.

The position or location of the plaques in relation to the artery wall can be accurately assessed in terms of eccentric (Figure 6) or concentric appearance or luminal changes regarding the involvement of the superior or inferior portion of the wall. On 3DIE, the majority of the calcified plaques appear as smooth protruding signs, as shown in Figure 7. The presence of heavily calcified plaques along the coronary artery, on the other hand, may result in irregular intraluminal changes in the coronary wall.

Figure 8 depicts visualization of a patient with extensive calcification at the RCA, LM, LAD, and LCX and irregular intraluminal appearances in the coronary wall.

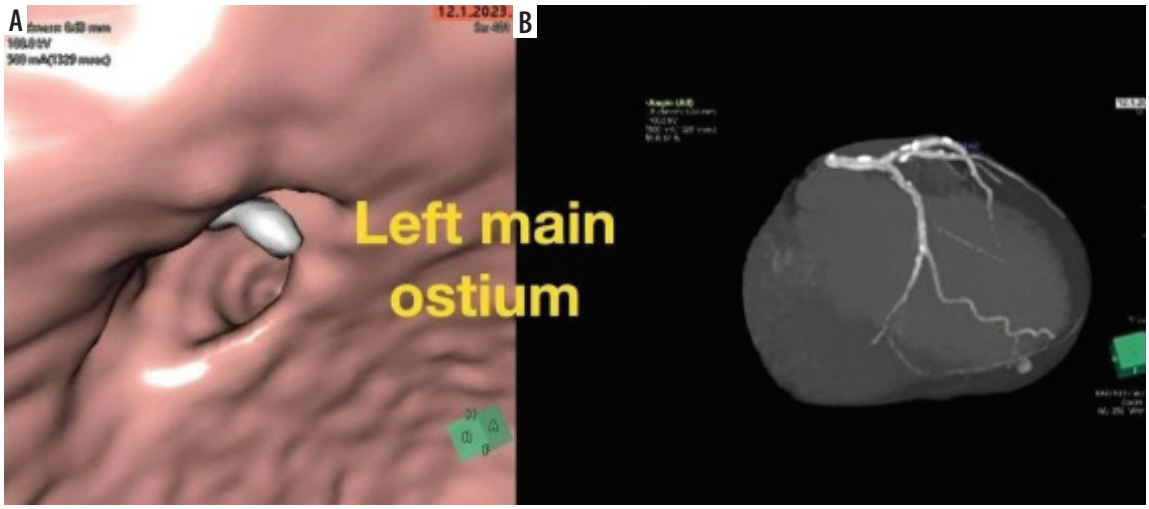

Figure 6. 3D IE visualization of eccentric calcified plaque. 3D IE shows the calcified plaque arising from the superior wall of LAD with involvement of LAD ostium. 3D reformatted image reveals calcified plaques at the left main stem and LAD coronary arteries in a 68-year-old male

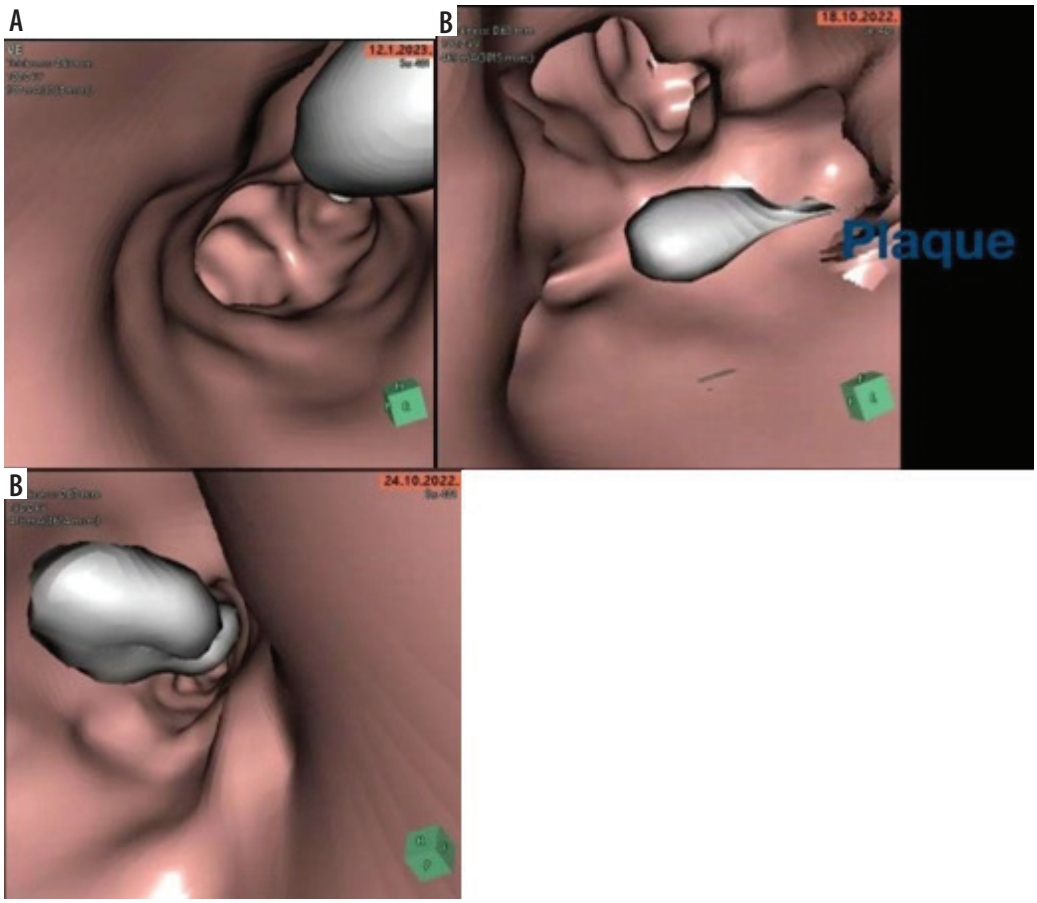

Figure 7. 3D IE visualization of eccentric calcified plaques

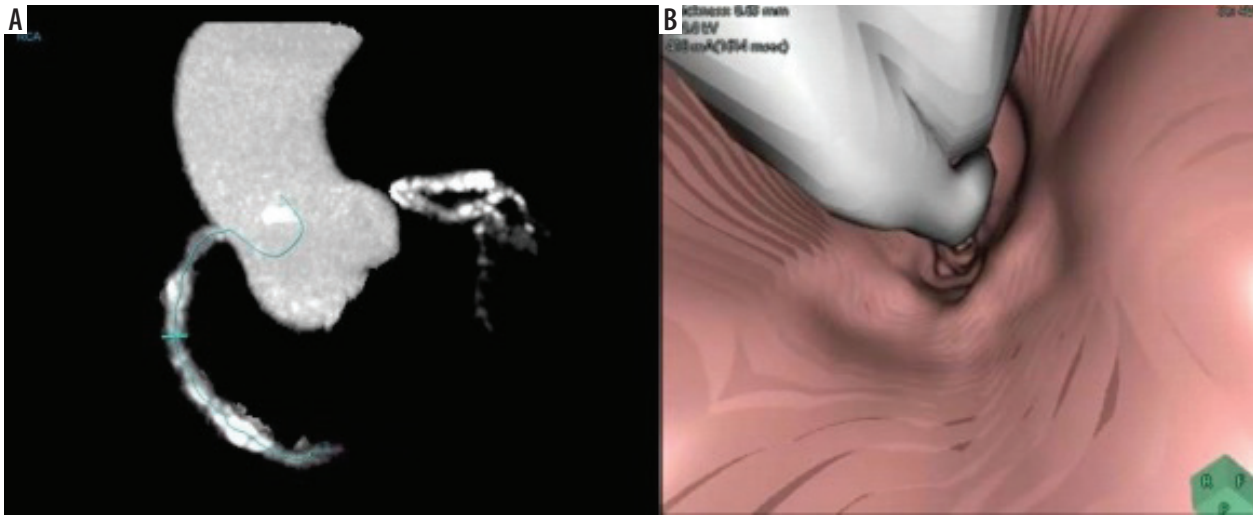

Figure 8. 3D IE visualization of extensively calcified plaques. 3D reformatted image shows extensively calcified plaques in the RCA, LM, LAD, and LCX in a 54-year-old male (**A**). Corresponding 3D IE demonstrates irregular coronary lumen changes caused by the extensively calcified plaques (**B**)

Mixed plaques

Because the plaques contain different components, irregular intraluminal appearances are common. This suggests that the coronary wall goes through several stages of remodeling, including a stable stage involving the formation of calcified plaques and an unstable stage involving the deposition of non-calcified plaques containing lipid-rich components. Figure 9 depicts mixed plaques at the proximal segment of the LAD, with the noncalcified component accounting for the majority of the content, and the corresponding (3DIE) demonstrating irregular intraluminal changes in the coronary wall caused by the mixed plaques.

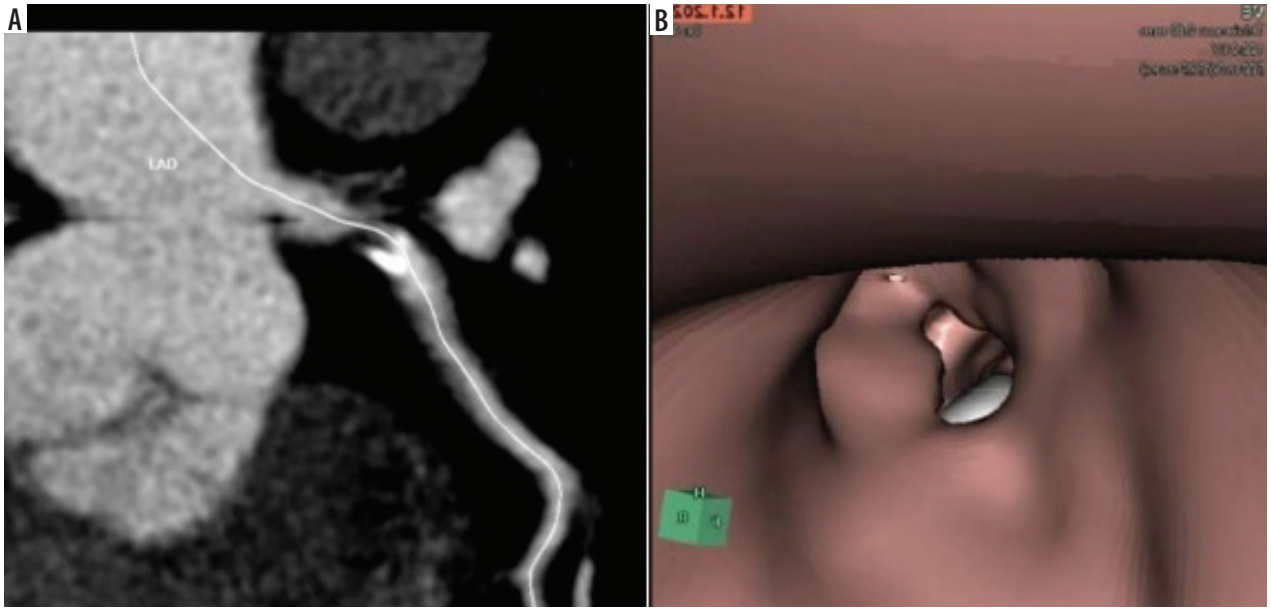

Figure 9. 3D IE visualization of mixed plaques. 3D reformatted image shows mixed plaques with spotty calcification at the proximal segment of LAD in a 63-year-old male. 3D IE indicates irregular coronary wall changes due to different components within the plaques

3DIE visualization of coronary stents

3DIE visualization has been reported to be a potential tool for endovascular stent grafting and stenting follow-up because it allows for the demonstration of intraluminal views of the artery wall and stent surface [15-20].

Standard stent appearances

Because CT attenuation of coronary stents is much higher than that of contrast-enhanced blood, stents can be easily visualized on 3DIE as a high-density structure with a uniform appearance inside the coronary arteries, depending on where the stents are deployed. On 3DIE visualization, Figure 10 depicts a patent coronary stent placed in the left anterior descending artery (LAD) with a smooth circular appearance.

Summary and conclusions

We have shown a spectrum of 3DIE findings of coronary plaques and coronary stents in this pictorial essay, which includes both normal lumen appearances and pathological changes caused by plaques or stents. Although 3DIE is not recommended as a routine tool for the detection of coronary plaques or stents, it can be used in conjunction with conventional visualizations to provide an accurate assessment of coronary plaques and stents.

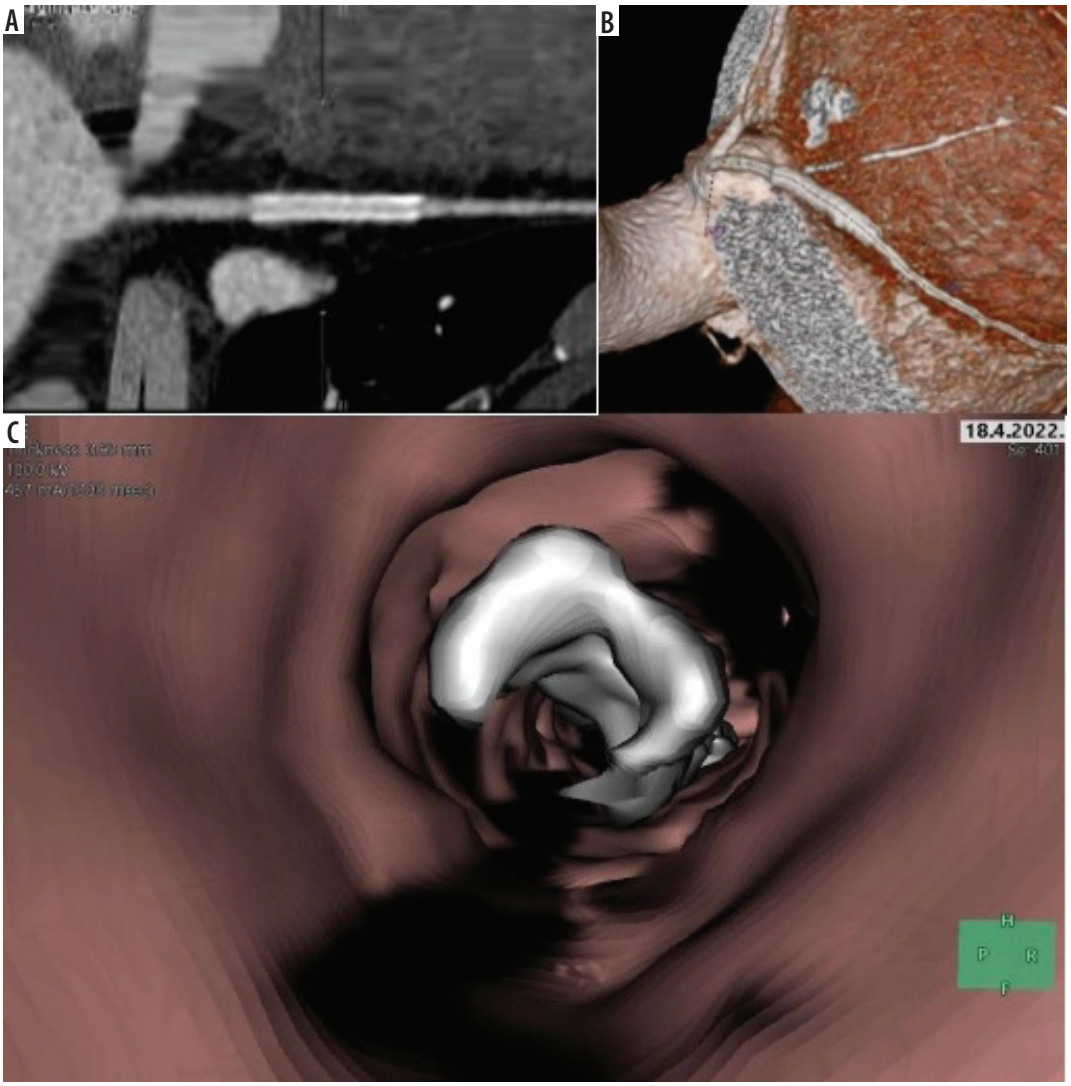

Figure 10. Visualization of functional coronary stents using 3D IE. **A**) A curved planar reformatted picture reveals a 56-year-old man's patent coronary stent in the LAD. **B**) Coronary stent visualization using VR. **C**) Stent surface close-up visualization on the 3D IE reveals a smooth, circular look inside the RCA

3DIE visualization has potential applications in the assessment of coronary plaques in terms of plaque characterization and intraluminal appearance, while in coronary stenting 3DIE can demonstrate intraluminal coronary stents in relation to coronary ostia or detect luminal changes due to in-stent restenosis.

3DIE visualization is believed to be useful for better understanding the effect of coronary plaques and stents on the coronary wall and subsequent clinical outcomes [12,13,15].

This review's 3DIE visualization tool could help overcome some of the image processing limitations for quantitative assessment of atherosclerotic plaques [20]. The table summarizes the main benefits of 3DIE visualization, but more research is needed to confirm the 3DIE findings and their associated clinical value.

Conflict of interest

The authors report no conflict of interest.

References

1. Schuijf JD, Beck T, Burgstahler C, et al. Differences in plaque composition and distribution in stable coronary artery disease versus acute coronary syndromes; non-invasive evaluation with multislice computed tomography. Acute Card Care 2007; 9: 48-53.
2. Vanhoenacker PK, Heijenbrok-Kal MH, Van Heste R, et al. Diagnostic performance of multidetector CT angiography for assessment of coronary artery disease: meta-analysis. Radiology 2007; 244: 419-428.
3. Sun Z, Lin CH, Davidson R, et al. Diagnostic value of 64-slice CT angiography in coronary artery disease: a systematic review. Eur J Radiol 2008; 67: 78-84.
4. Abdulla J, Abildstrom SZ, Gotzsche O, et al. 64-multislice detector computed tomography coronary angiography as potential alternative to conventional coronary angiography: a systematic review and metaanalysis. Eur Heart J 2007; 28: 3042-3050.
5. Sun ZH, Cao Y, Li HF. Multislice computed tomography angiography in the diagnosis of coronary artery disease. J Geriatr Cardiol 2011; 8: 104-113.
6. Rodriguez-Granillo GA, Rosales MA, Degrossi E, et al. Multislice CT coronary angiography for the detection of burden, morphology and distribution of atherosclerotic plaques in the left main bifurcation. Int J Cardiovasc Imaging 2007; 23: 389-392.
7. Schmid M, Pflederer T, Jang IK, et al. Relationship between degree of remodeling and CT attenuation of plaque in coronary atherosclerotic lesions: an in-vivo analysis by multi-detector computed tomography. Atherosclerosis 2008; 197: 457-464.
8. Motoyama S, Kondo T, Sarai M, et al. Multislice computed tomographic characteristics of coronary lesions in acute coronary syndromes. J Am Coll Cardiol 2007; 50: 319-326.
9. Van Ooijen PMA, Nieman K, De Feyter PJ, et al. Noninvasive coronary angioscopy using electron beam computed tomography and multidetector computed tomography. Am J Cardiol 2002; 90: 998-1002.
10. Schroeder S, Kopp AF, Ohnesorge B, et al. Virtual coronary angioscopy using multislice computed tomography. Heart 2002; 87: 205-209.
11. Sun Z, Zheng H. Effect of suprarenal stent struts on the renal artery with ostial calcification observed on CT virtual intravascular endoscopy. Eur J Vasc Endovasc Surg 2004; 28: 534-542.
12. Sun Z, Dimpudus FJ, Nugroho J, et al. CT virtual intravascular endoscopy assessment of coronary artery plaques: a preliminary study. Eur J Radiol 2010; 75: e112-e119. doi: 10.1016/j.ejrad.2009.09.007.
13. Sun Z. 3D multislice CT angiography in post-aortic stent grafting: a pictorial essay. Korean J Radiol 2006; 7: 205-211.
14. Sun Z, Allen YB, Nadkarni S, et al. CT virtual intravascular endoscopy in the visualization of fenestrated stent-grafts. J Endovasc Ther 2008; 15: 42-51.
15. Sun Z, Cao Y. Multislice CT angiography assessment of left coronary artery: correlation between bifurcation angle and dimensions and development of coronary artery disease. Eur J Radiol 2011; 79: e90-e95. doi: 10.1016/j.ejrad.2011.04.015.
16. Kopp AF, Ohnesorge B, Flohr T, et al. Cardiac multidetector-row CT: first clinical results of retrospectively ECG-gated spiral with optimized temporal and spatial resolution. Rofo 2000; 172: 429-435. doi: 10.1055/s-2000-673.
17. Jodas DS, Pereira AS, Tavares JMRS. A review of computational methods applied for identification and quantification of atherosclerotic plaques in images. Expert Syst Appl 2016; 46: 1-14.
18. Sun Z, Al Dosari SA, Ng C, et al. Multislice CT virtual intravascular endoscopy for assessing pulmonary embolisms: a pictorial review. Korean J Radiol 2010; 11: 222-230.
19. Sun Z. Coronary CT angiography in coronary artery disease: correlation between virtual intravascular endoscopic appearances and left bifurcation angulation and coronary plaques. Biomed Res Int 2013; 2013: 732059. doi: 10.1155/2013/732059.
20. Ohnesorge B, Flohr T, Becker C, et al. Cardiac imaging by means of electrocardiographically gated multisection spiral CT: initial experience. Radiology 2000; 217: 564-571.